SETAC PRESS

Environmental Toxicology and Chemistry, Vol. 36, No. 2, pp. 346–353, 2017

Printed in the USA

FOURIER-TRANSFORM INFRARED SPECTROSCOPY AS A NOVEL APPROACH TO PROVIDING EFFECT-BASED ENDPOINTS IN DUCKWEED TOXICITY TESTING

Li-Xin Hu,† Guang-Guo Ying,*† Xiao-Wen Chen,† Guo-Yong Huang,† You-Sheng Liu,† Yu-Xia Jiang,† Chang-Gui Pan,† Fei Tian,† and Francis L. Martin‡

†State Key Laboratory of Organic Geochemistry, Guangzhou Institute of Geochemistry, Chinese Academy of Sciences, Guangzhou, China
‡Centre for Biophotonics, Lancaster Environment Centre, Lancaster University, Lancaster, United Kingdom

(Submitted 9 March 2016; Returned for Revision 21 April 2016; Accepted 17 June 2016)

Abstract: Traditional duckweed toxicity tests only measure plant growth inhibition as an endpoint, with limited effects-based data. The present study aimed to investigate whether Fourier-transform infrared (FTIR) spectroscopy could enhance the duckweed (*Lemna minor* L.) toxicity test. Four chemicals (Cu, Cd, atrazine, and acetochlor) and 4 metal-containing industrial wastewater samples were tested. After exposure of duckweed to the chemicals, standard toxicity endpoints (frond number and chlorophyll content) were determined; the fronds were also interrogated using FTIR spectroscopy under optimized test conditions. Biochemical alterations associated with each treatment were assessed and further analyzed by multivariate analysis. The results showed that comparable *x*% of effective concentration (EC*x*) values could be achieved based on FTIR spectroscopy in comparison with those based on traditional toxicity endpoints. Biochemical alterations associated with different doses of toxicant were mainly attributed to lipid, protein, nucleic acid, and carbohydrate structural changes, which helped to explain toxic mechanisms. With the help of multivariate analysis, separation of clusters related to different exposure doses could be achieved. The present study is the first to show successful application of FTIR spectroscopy in standard duckweed toxicity tests with biochemical alterations as new endpoints. *Environ Toxicol Chem* 2017;36:346–353. © 2016 SETAC

Keywords: Biochemical fingerprint Biospectroscopy Duckweed Fourier-transform infrared spectroscopy Multivariate analysis Toxicity test

INTRODUCTION

In (eco)toxicological research, toxic effects are determined based on estimation of various endpoints, a time-consuming aspect of many tests [1,2]. Traditional toxicological endpoints often involve the examination of lethality or inhibition of the test organism, and physical characteristics [3–5]. Alterations in biomarkers, including lipids, proteins, nucleic acids, and carbohydrates, may also be used as endpoints in toxicity tests [6,7].

As a useful tool, infrared spectroscopy can provide detailed biochemical information, including lipids, proteins, deoxyribonucleic acid/ribonucleic acid (DNA/RNA), and carbohydrates of a biological sample [8]. Alterations in secondary structure of proteins, protein phosphorylation, can also be identified in the vibrations of functional groups of the biomaterials [9,10]. So far, this tool has been used to diagnose disease, especially as an emerging, simple, and nondestructive tool in cancer diagnosis [11–13]. Infrared spectroscopy can also be used in various fields such as forensic casework, biome identification, and metabolomics stress response [14–18]. Even though the infrared spectrum has been widely used in various biological materials such as cells and tissues, comparative analysis between attenuated total reflectance (ATR) and transmission has been lacking [19].

Fourier-transform infrared (FTIR) spectroscopy is emerging as a sensor-based tool for correlating the structure of biomolecules in different biological systems [20]. As different chemical bonds of biochemical samples absorb light in the mid-infrared region (including 3000–2800 cm^{-1} and 1800–900 cm^{-1}), the application of FTIR spectroscopy may help to determine the chemical structure of molecules in biochemical samples [15]. A vibrational spectrum is generated, and the region of 1800 cm^{-1} to 900 cm^{-1} is often known as a biochemical fingerprint [21,22]. The infrared spectra generated from analysis as a dataset can be considered in a multidimensional space, and the dimensionality is best reduced using sophisticated multivariate analysis techniques such as principal component analysis and linear discriminant analysis, which capture the most important variations [21,23,24]. Considering its advantages (biochemical fingerprinting, sample nondestructive, and simple operation features), FTIR may be used as a powerful tool in ecotoxicity testing.

The purpose of the present study was to investigate whether FTIR spectroscopy can be applied in a standard ecotoxicity test using 4 test agents (Cu, Cd, atrazine, and acetochlor as the representatives of metals and herbicides) and 4 industrial wastewater samples with duckweed used as the test species. Following exposure of duckweed to the chemicals, standard toxicity endpoints (growth inhibition) were determined, while fronds were interrogated using FTIR spectroscopy under optimized test conditions. Biochemical alterations associated with each treatment were assessed and analyzed by multivariate analysis. These results may validate the application of FTIR spectroscopy in the interpretation of toxic effects.

MATERIALS AND METHODS

Chemical agents

Four chemicals (Cu, Cd, atrazine, and acetochlor) were selected as the test agents. Both $CuSO_4$ and $CdCl_2$ (purity >99%) were purchased from XILONG Chemical, whereas atrazine and acetochlor (purity >99.9%) were obtained from Dr. Ehrenstorfer.

This article includes online-only Supplemental Data.

* Address correspondence to guang-guo.ying@gig.ac.cn; guangguo.ying@gmail.com

Published online 22 June 2016 in Wiley Online Library (wileyonlinelibrary.com).

DOI: 10.1002/etc.3534

Methanol and ethanol (Merck) were high-performance liquid chromatography (HPLC). Stock solutions of $CuSO_4$, $CdCl_2$, and acetochlor were prepared by dissolving the compounds in Milli-Q water at concentrations of 10 000 mg/L, 10 000 mg/L, and 100 mg/L, respectively, whereas the stock solution of atrazine was predissolved in methanol at 1000 mg/L. All other chemical reagents used were of HPLC or analytical grade.

The components of a modified Swedish Standards Institute medium [25] are as follows: 75 mg/L $MgSO_4 \cdot 7H_2O$, 85 mg/L $NaNO_3$, 36 mg/L $CaCl_2 \cdot 2H_2O$, 20 mg/L $NaCO_3$, 13.4 mg/L KH_2PO_4, 1.0 mg/L H_3BO_3, 0.2 mg/L $MnCl_2 \cdot 4H_2O$, 0.01 mg/L $Na_2MoO_4 \cdot 2H_2O$, 0.05 mg/L $ZnSO_4 \cdot 7H_2O$, 0.005 mg/L $CuSO_4 \cdot 5H_2O$, 0.01 mg/L $Co(NO_3)\ 2 \cdot 6H_2O$, 0.84 mg/L $FeCl_3 \cdot 6H_2O$, and 1.4 mg/L Na_2 ethylenediamine tetraacetic acid. All substances in the medium were prepared in Milli-Q water, and the pH was adjusted to 6.5 ± 0.2 by addition of NaOH or HCl solution.

Test species

Duckweed *Lemna minor* L. was used in the experiments. It was cultured for 1 mo as a preculture in the laboratory in the Swedish Standards Institute medium under the following conditions: 2000 lux; $25 \pm 1\ ^{\circ}C$; 14:10-h light:dark cycle; humidity 60%. The medium was replaced every 2 wk.

Duckweed exposure experiments

Range finding test. Duckweed toxicity tests were conducted in a series of 6-well plates. Each well contained 10 mL of the Swedish Standards Institute medium and 4 colonies with approximately the same size of 3-frond *L. minor*. Six concentrations (0 mg/L, 0.0001 mg/L, 0.001 mg/L, 0.01 mg/L, 0.1 mg/L, 1 mg/L, or 10 mg/L) for each test compound were used in the range-finding test, and each treatment was replicated 3 times. Plants were maintained under the conditions given above in *Test species*. The number of fronds in each well was counted every 48 h. After 96-h exposure to chemicals, plants were picked out for analysis of biomass and chlorophyll content.

Test conditions determined. Test conditions, including fixing methods and instrumental parameters, were optimized using the following design.

The experiment was set up at the same exposure conditions for Cu as the test agent at a concentration of an approximate median effective concentration (EC50) value based on the range-finding test results, and for the control without Cu. After exposure, the fronds of the control groups and Cu treatment groups were fixed with multiple methods for plant samples, including (A) 70% ethanol, (B) 0.9% NaCl, (C) 10% formalin in phosphate-buffered saline, and (D) Conroy solution. After 12 h, the fixed samples were tiled on BaF2 glass slides, and dried in the desiccator for at least 24 h. Then the samples were interrogated using FTIR with ATR and transmission modes.

Exposure to chemicals. Once the approximate EC50 value for each test agent was obtained, the exposure experiment could be set up at a range of concentrations. The exposure concentrations of Cu, Cd, and acetochlor were diluted with Milli-Q water whereas the exposure concentrations of atrazine were diluted with methanol from the stock solutions. Ten μL of each test agent were delivered in each well with 10 mL of medium. Because the methanol solvent may affect the toxic effects [26], the accessory solvent of the atrazine treatment group was dried before 10 mL of medium was added to each well. Then 4 precultured duckweed plants, each with 3 fronds, were selected for chemical exposure. The number of fronds in each well was counted every 48 h. After 96 h of exposure, several fronds were fixed with 10% (v/v) formalin and stored at room temperature until FTIR analysis.

The exposure concentrations were measured at intervals throughout the experiment by using atomic absorption spectrometry (Varian) for Cu and Cd, and HPLC for atrazine and acetochlor on an Agilent system equipped with an Eclipse XDB-C18 (5 μm, 4.6 mm × 150 mm) column. The nominal and measured concentrations of the agents were not significantly different, except for copper, because of an instrument systematic error (Supplemental Data, Table S1).

Exposure to wastewater samples. Four wastewater samples were collected in a wastewater treatment plant of an electroplate factory in southern China, including: A, influent with a high concentration of copper; B, effluent with copper as the main component; C, influent with a high concentration of chromium; and D, effluent with mixed metals. All wastewater samples were filtered through glass fiber filters (Whatman GF/F, 0.7-μm effective pore size), and 2-fold diluted with the Swedish Standards Institute medium (100%, 50%, 25%, 12.6%, 6.25%, and 3.125%). Then those solutions were used for duckweed toxicity tests with the same conditions as the 4 test agents. The metal concentrations were measured by atomic absorption spectrometry.

Traditional duckweed toxicity test endpoints

Following each exposure treatment, plant growth inhibition was calculated using the frond number and chlorophyll content. The fronds of duckweed were picked out carefully and placed on blotting paper for several minutes. Then all fronds from all treatments were weighed and placed into a 2-mL centrifuge tube with 2 mL 95% (v/v) ethanol for 48 h.

The supernatant was used for chlorophyll a (Ca), chlorophyll b (Cb), and Ca+b (Ca+Cb) estimation. Absorbance at 663 nm and 645 nm was measured using a microplate reader (BMG Labtech FLUOstar Omega), and the chlorophyll content was obtained by a previous method [27]. The percentage of inhibition of plant growth compared with the control was calculated according to a previously published protocol [25].

FTIR spectral measurement and analysis

Duckweed plants fixed with 10% (v/v) formalin were washed 3 times with phosphate-buffered saline and water in sequence, then spread onto BaF2 slides and dried in the desiccator for at least 24 h. The prepared samples on BaF2 slides were investigated using a Bruker Vector 70 FTIR spectrometer (Bruker Optics) equipped with a HYPERION microscope, which contained a liquid nitrogen-cooled detector. The instrumental settings were optimized: transmission mode, 64 scans, and 8 cm^{-1} resolution. At different positions of the dried frond samples, 25 spectra from each sample were acquired. Prior to starting the next slide, a background spectrum was taken for background noise subtraction.

Data preprocessing and multivariate analysis

Raw infrared spectra obtained from the samples were analyzed using the irootlab toolbox [28] running on Matlab r2010a. Each spectrum was cut at the biochemical fingerprint region (1800–900 cm^{-1}) and C-H stretching region (3000–2800 cm^{-1}), followed by rubber-band baseline correction, and normalization to the amide I peak ($\sim$1650 cm^{-1}) in the biochemical fingerprint region and to the maximum in the C-H stretching region ($\sim$2920 cm^{-1}) [21]. Following this preprocessing, principal component analysis and/or linear discriminant analysis was

applied to each dataset separately, to identify biochemical alterations that segregate treated groups from each other [15]. To reduce the dimensions of the datasets, principal component analysis was applied to the spectral dataset [29], whereas linear discriminant analysis was applied to discriminate treated groups [15,30].

In score plots, nearness in the first linear discriminant analysis factor (LD1) between samples indicates the similarity of toxic effects, whereas distance means difference [15]. Dose–response curves were derived based on the distance between each treatment mean and the control mean in the LD1 space.

Statistical analysis

Data on duckweed growth inhibition are presented as mean ± standard deviation (SD) in each treatment; they were analyzed for statistical differences by analysis of variance (ANOVA). All ANOVA tests were performed in GraphPad Prism 4 (GraphPad Software). Dose–response curves were fitted with the logistic model. Pearson correlation analysis was performed with SAS 9.1 software (SAS Institute).

RESULTS AND DISCUSSION

Optimization of sample processing method and instrumental conditions

Before duckweed toxicity testing, test conditions were optimized, mainly for the fixative and FTIR instrumental conditions. A typical infrared spectrum of the fronds of duckweed derived from the FTIR spectroscopy is shown in the Supplemental Data, Figure S1. The datasets generated from the FTIR analysis are complex and multidimensional. No obvious differences between different treatment groups could be readily observed throughout the selected spectral C-H stretching region (3000–2800 cm^{-1}) and the biochemical fingerprint region (1800–900 cm^{-1}). Given the large numbers of spectra generated, computational analyses including principal component analysis and linear discriminant analysis were thus applied to discriminate treatment groups and distinguish correlative biomarkers contributing to variance.

Four fixing solutions (A, 70% ethanol; B, 0.9% NaCl; C, 10% formalin in phosphate-buffered saline; and D, Conroy solution) and 2 instrumental modes (ATR mode vs transmission mode) were compared with an optimized test method for application in the toxicity characterization. Because the ATR mode is mainly applied to homogeneous samples, it primarily expresses the surface information of the tissues if the sample is thick. In fact, infrared can penetrate duckweed fronds, so the transmission mode would better reflect the toxic effects inside plant cells than the ATR mode. The cluster vector plots demonstrated this difference (Supplemental Data, Figure S2).

Among the 4 fixing solutions, the cluster for solution B (0.9% NaCl) segregated away from those for the other 3 solutions in both the control and the Cu-treated group under the ATR and transmission modes (Supplemental Data, Figure S2). As the cluster vector plots show in the Supplemental Data (Figure S2, bottom), the duckweed fronds treated with this solution showed biochemical alterations of lipid and protein structures during the drying process. It was also observed that Conroy solution (D) might induce alterations in lipids and proteins. Solution A (70% ethanol) showed few variations in the Cu-treated group, but it induced several changes in the C-H stretching region in the control group because of its lipid-soluble nature. In comparison to the other 3 solutions, solution C (10% formalin in phosphate-buffered saline) induced fewer alterations in both ATR mode and transmission mode for the control group and the chemical-treated group.

Both ethanol and formaldehyde are common fixatives with different reactions [31]. Because its molecular structure is similar to water, ethanol competes for protein hydrogen bonds with water to replace the water molecules in its organization; the protein precipitates in the isoelectric point by reducing the protein-bound electric constant and blocks the antibodies–epitope combination [32]. Alcohols can also dissolve the lipid materials, and have weak penetration, as they form a layer of membrane protein that may block fixed liquid penetration and cause the intermediate organization to be poorly fixed [33,34]. Thus ethanol is sometimes not a good fixative for certain biological samples. In contrast, formaldehyde is the most common fixative for retaining tissue and cell protein targets as it depends on the formation of cross-linked protein–protein and protein-containing methylene (CH2-) nucleic acids [35]. Thus solution C (10% formalin in phosphate-buffered saline) was selected as fixative for FTIR analysis of fronds under the transmission mode.

Effects of duckweed exposure to chemicals

Following exposure of duckweed to the 2 metals (Cu and Cd) and 2 pesticides (atrazine and acetochlor), the dose–response curves were obtained for each chemical based on traditional toxicity endpoints (Supplemental Data, Figure S3) and FTIR spectroscopy (Figure 1). General observations of the toxic effects on duckweed following exposure to the 4 chemicals are given in the Supplemental Data, Table S2, whereas distinct FTIR peak assignments at different exposure concentrations are presented in the Supplemental Data, Table S3. Various effective concentrations (EC*x*: EC1, EC10, and EC50) for the 4 chemicals were calculated based on the endpoints of plant growth rate inhibition, total chlorophyll inhibition at 96 h, and alterations in the biochemical fingerprint region (1800–900 cm^{-1}) and C-H stretching vibration region (3000–2800 cm^{-1}) along the LD1 space (Table 1). When compared with the traditional endpoints, generally comparable results were achieved from FTIR spectroscopy. The EC50 values for Cu, Cd, atrazine, and acetochlor based on principal component analysis and/or linear discriminant analysis results of the biochemical fingerprint region were 0.198 mg/L, 0.673 mg/L, 0.0302 mg/L, and 0.0028 mg/L, whereas the EC50 values for duckweed growth inhibition (I_{96h}) were 0.157 mg/L, 1.27 mg/L, 0.0405 mg/L, and 0.00410 mg/L, respectively (Table 1). Overall, statistically significant correlations existed between the phenotypic and the biochemical alterations (Supplemental Data, Table S5). Specifically, significant correlations have been found among the growth inhibition rate, total chlorophyll, and biochemical alterations for the metal groups and herbicide group ($R^2 > 0.9$, $p < 0.05$). This suggests the applicability of FTIR spectroscopy in duckweed toxicity testing, and the availability of additional biochemical alteration information.

Treatment of duckweed with the chemicals showed increased alterations of biomolecules with chemical exposure concentrations (Figure 2; Supplemental Data, Table S2). For Cu, the main alterations associated with the EC50 dose included vibrations related to glycogen (~1000 cm^{-1}), amide I (~1600 cm^{-1}), amide II (~1540 cm^{-1}), amino acid residues (~1405 cm^{-1}), and protein phosphorylation (~950 cm^{-1}; Figure 2). When low-dose and high-dose exposures were compared, discriminating loadings throughout the biochemical fingerprint region were observed. The observed toxic effects

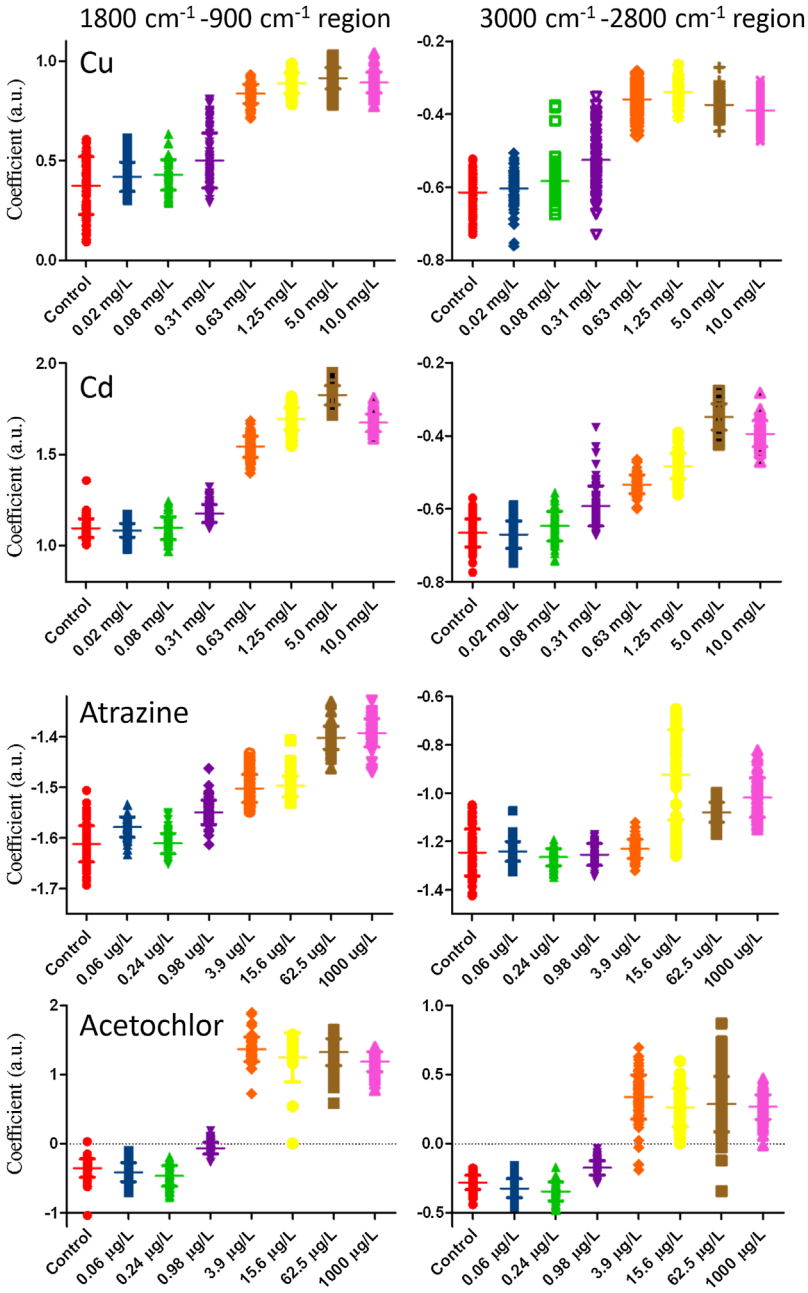

Figure 1. Dose–response curves showing effects of duckweed exposure to various doses of Cu, Cd, atrazine, and acetochlor (96 h) based on Fourier-transform infrared spectroscopy. Principal component analysis–linear discriminant analysis score plots and the resultant cluster vectors were derived from triplicate experiments ($n = 75$ spectra per chemical treatment). Panels in the left column represent infrared alterations concentrated in the biochemical fingerprint region (1800–900 cm^{-1}); those in the right column were concentrated in the lipid region (3000–2800 cm^{-1}). Each symbol indicates 1 independent experiment containing an average of 25 separated infrared spectra per slide. See Figure 2 for the legend.

were associated with alterations to lipids (~1740 cm^{-1}) and nucleic acids (~1080 cm^{-1}) at high doses, and to carbohydrate (~1140 cm^{-1}) and amide III (~1260 cm^{-1}) at low doses. The results of the present study showed that Cu affected the protein in organisms through combining with protein molecules and amino acids. As an essential element, Cu can be incorporated into various enzymes that perform essential metabolic functions [36]. Copper can also exist in oxidized or reduced forms in living cells, and it acts as a catalyst in the production of reactive oxygen species, which can cause oxidative damage and induce adverse effects [37–39]. In addition, Cu can also result in pernicious effects on chlorophyll, so chlorophyll may be more sensitive than frond number and biomass [40].

Cadmium produced different biochemical alterations than Cu in duckweed (Figure 2). The biochemical alterations induced by Cd were associated with amide II (~1550 cm^{-1}), amide III (~1315 cm^{-1}), lipids (~1740 cm^{-1}), and nucleic acids (~1080 cm^{-1}). The low-dose treatments did not cause significant alterations at coefficient in cluster vectors. However, the high-dose treatments brought out discriminating loadings at amide I (~1650 cm^{-1}), lipids (~1740 cm^{-1}), amino acid residues (~1400 cm^{-1}), nucleic acids (~1080 cm^{-1}), and glycogen (~1050 cm^{-1}). Cadmium may induce lipid peroxidation and changes to the antioxidant system [41]. It combines easily with –OH, –NH2, and –SH groups in protein [42,43]. It can cause conformational changes to membrane proteins, thus

Table 1. The effective concentration values of different chemicals

	NOEC (EC1; mg/L)				LOEC (EC10; mg/L)				EC50 (mg/L)			
	I_{96h}[a]	CI[b]	P1[c]	P2[d]	I_{96h}[a]	CI[b]	P1[c]	P2[d]	I_{96h}[a]	CI[b]	P1[c]	P2[d]
Cu	0.0058	0.0018	0.0006	0.0004	0.0256	0.0117	0.008	0.0092	0.157	0.114	0.198	0.418
Cd	0.0861	0.0049	0.0415	0.0165	0.289	0.0345	0.145	0.103	1.27	0.379	0.673	0.969
Atrazine	0.003	0.0025	0.0001	0.0003	0.0097	0.0129	0.0013	0.0059	0.0405	0.0959	0.0302	0.256
Acetochlor	0.0001	–[e]	–[e]	–[e]	0.0005	0.0003	0.0001	0.0002	0.00410	0.0039	0.0028	0.003

[a]Growth rate inhibition at 96 h.
[b]Total chlorophyll inhibition (CI).
[c]Principal component analysis–linear discriminant analysis (PCA–LDA) results of biochemical fingerprint region (1800–900 cm−1).
[d]PCA–LDA results of C-H stretching vibrations (lipid region 3000–2800 cm^{-1}).
[e]Data were below 0.0001.
EC = effective concentration; NOEC = no-observed-effect concentration; LOEC = lowest-observed-effect concentration; P1 = principal component 1; P2 = principal component 2.

affecting membrane lipid fluidity and changing the function of membrane protein and liquidity, leading to damage to membrane lipids [44]. Cadmium can also replace the function of Zn in the body, can damage Zn-containing enzyme functions, which relate to respiratory and other physiological processes, and finally can inhibit the growth of plants and lead to death [45].

For atrazine, the main biochemical alterations in duckweed of the low-dose treatments were related to amide I (∼1650 cm^{-1}), which is concerned with the secondary structure of protein, and carbohydrate (∼1000 cm^{-1}). At the doses above a toxic unit, changes occurred in proteins and lipids, which became more obvious with increasing doses. In addition, the alterations associated with nucleic acids (∼1080 cm^{-1}) and carbohydrate (∼1150 cm^{-1}) were also observed in duckweed. Atrazine mainly destroys photosynthesis, and it can also disturb a plants hormone and iron balance, leading to collapse of the metabolism and thus affecting synthesis of RNA, enzymes, and proteins [46].

For acetochlor, the biochemical alterations at low doses were associated with protein secondary structure (∼1650 cm^{-1}), amide II (∼1540 cm^{-1}), carbohydrate (∼1180 cm^{-1}), and glycogen (∼1030 cm^{-1}). At high doses, the biochemical alterations showed distinguishing wavenumbers associated with amide II (∼1535 cm^{-1}), amide I (∼1650 cm^{-1}), asymmetric phosphate (∼1226 cm^{-1}), carbohydrate (∼1030 cm^{-1}), and protein phosphorylation (∼995 cm^{-1}). The toxic mechanism for acetochlor in plants is mainly through inhibition of cell growth, causing the plants to stop growing by blocking protein synthesis [47].

The 2-dimensional score plots of the biochemical region (1800–900 cm^{-1}) showed different segregation patterns from the control and their wavenumber basis (Figure 3; Supplemental Data, Figures S4 and S5). The results from the present study clearly showed that different chemicals induced diverse alterations at the same toxic dose because of their different toxic mechanisms. Thus, bio-spectroscopy not only showed the toxic effects in duckweed induced by chemicals at varying

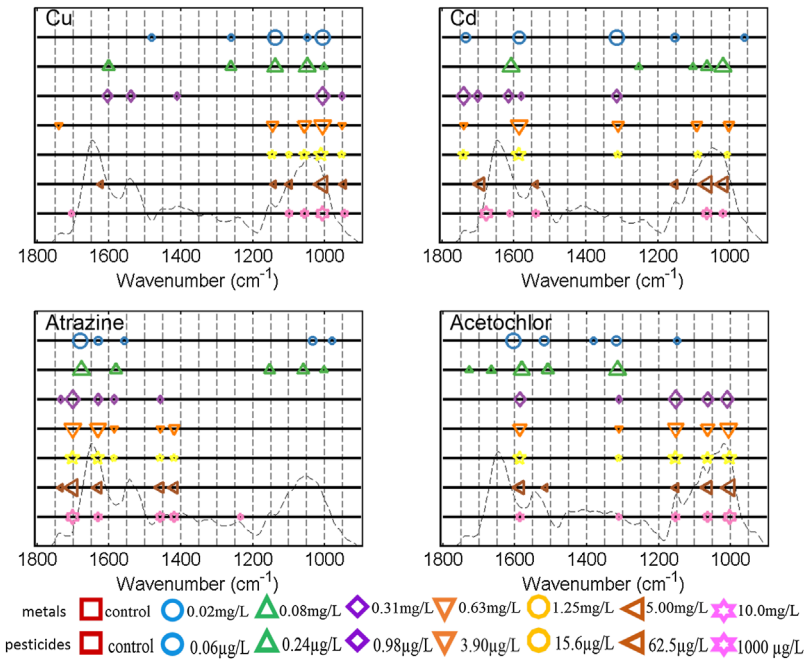

Figure 2. Peak plots of cluster vectors indicating the wavenumber basis for segregation following treatment of fronds with the chemicals. Each treatment is compared with the control. The size of the symbol in the plot is proportional to the height of the corresponding peaks, which are relative to the extent of biochemical alterations compared to the control. The black horizontal line represents the control. The dotted line represents a typical infrared spectrum of the biochemical fingerprint region (1800–900 cm^{-1}). Note: Because the treated concentrations of metals were the same, Figures 1 and 2 share a legend and the same is true for the pesticides.

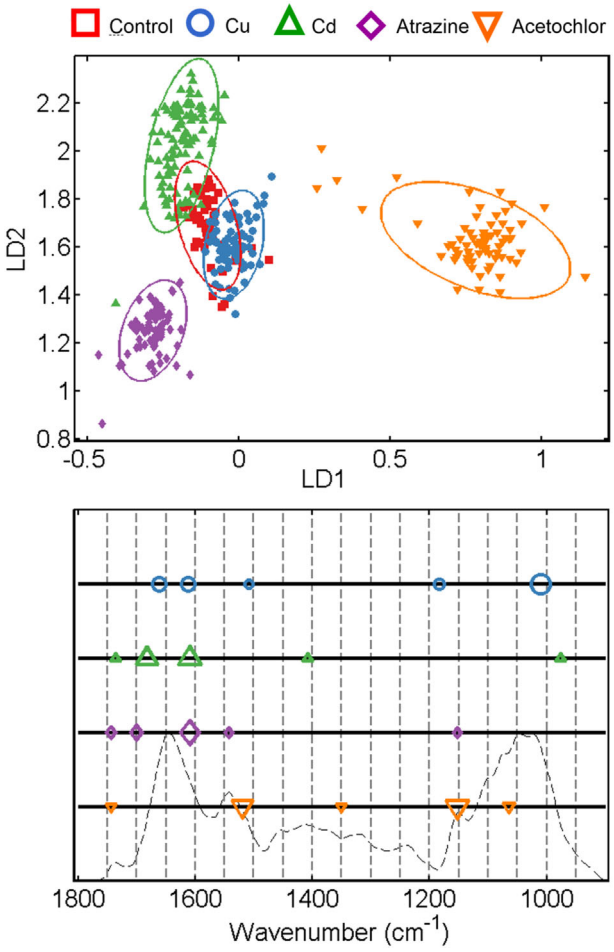

Figure 3. Principal component analysis–linear discriminant analysis score plots showing effects of the treatment of fronds with the chemicals at a toxic unit (median effective concentration [EC50]). **Top:** In the score plots in 2 dimensions (90% confidence ellipsoids) of the biochemical region (1800–900 cm^{-1}), peak plots of cluster vectors indicate the wavenumber basis for segregation following treatment of fronds. **Bottom:** The size of the symbol in the plot is proportional to the extent of biochemical alteration compared to the vehicle control. The dashed line represents a typical infrared spectrum of the biochemical fingerprint region (1800–900 cm^{-1}). LD = linear discriminant analysis factor.

concentrations, but also explained specific biochemical alterations.

FTIR spectroscopy application to wastewater toxicity test

The FTIR spectroscopy was also applied to the toxicity tests of 4 industrial wastewater samples. Wastewater samples A and C were influents, and samples B and C were effluents. Sample A contained mainly Cu (110 mg/L) and several other metals (Al, Fe, Cr, and Zn) at 2 mg/L to 10 mg/L, whereas sample B from the same wastewater treatment system contained only a low concentration of Cu (0.1 mg/L). Sample C mainly contained Cr (128 mg/L), whereas sample D contained various metals (Ni, Cu, and Zn) at concentrations of 3 mg/L to 5 mg/L. Growth inhibition was observed for the 2 influent samples even after dilution to 3.13%; but for the 2 effluent samples, growth inhibition was found only in 100% of sample B and 100% and 50% of sample C.

The results from FTIR spectroscopy analysis showed clear segregation of the influent samples (A and C) from the effluent samples (B and D) and the control (Figure 4). This suggests significant differences in biomolecular alterations induced by different wastewaters. Along the LD1, the major difference was induced by influent sample C with a high Cr concentration, whereas at the LD2, a difference was obvious for influent sample A with a high concentration of Cu. Cluster separation was not obvious between the control and effluents. In any case, there was a clear segregation between the influents and effluents, indicating large differences in toxicity.

Biochemical alterations observed in duckweed following exposure to the Cu-containing influent A were found in secondary structures associated with amide I (~1670 cm^{-1} and ~1640 cm^{-1}), DNA (~1225 cm^{-1}), and protein phosphorylation (~980 cm^{-1}; Figure 4). Effluent B caused major alterations in amide I (~1640 cm^{-1}), and minor changes in carbohydrate (~1000 cm^{-1}), nucleic acids (~1080 cm^{-1}), and amide II (~1520 cm^{-1}). The Cr-induced alterations for influent C were noted mainly in amide II (~1580 cm^{-1}), followed by amide III (~1320 cm^{-1}), as well as asymmetric phosphate stretching vibration in DNA (~1225 cm^{-1}). Changes in duckweed from

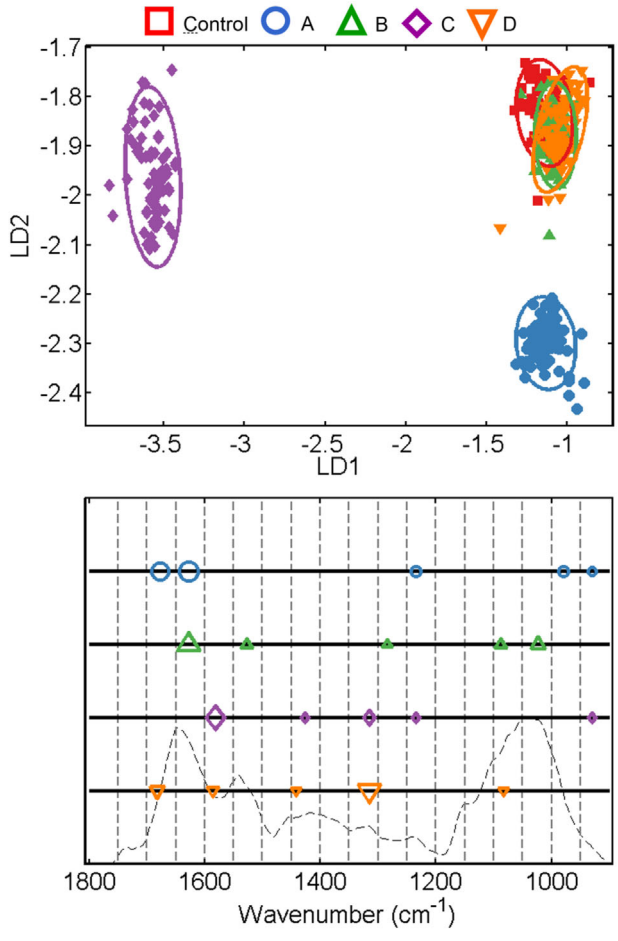

Figure 4. **Top:** Principal component analysis–linear discriminant analysis score plots of the biochemical region (1800–900 cm^{-1}) of duckweed following exposure to the wastewaters from a plating plant (A = the influent with a high concentration of copper; B = the effluent with a low concentration of copper; C = influent with a high concentration of chromium; D = the effluent with several metals at low concentrations). Confidence ellipsoids (90%) are drawn assuming a normal distribution in 3D scatter plots. Peak plots of cluster vectors indicate the wavenumber basis for segregation following treatment of fronds. **Bottom:** The size of the symbol in the plot is proportional to the extent of biochemical alteration compared to the vehicle control. LD = linear discriminant analysis factor.

exposure to effluent D were found mainly in amide III ($\sim$1310 cm^{-1}), followed by amide I ($\sim$1680 cm^{-1}), amide II ($\sim$1570 cm^{-1}), and nucleic acids ($\sim$1080 cm^{-1}). Biochemical alterations in duckweed induced by different contaminants could be used as a biomarker at the bio-macromolecular level for characterizing their biological mechanisms of toxicity.

In summary, the results indicate that FTIR spectroscopy can be applied in duckweed toxicity testing, and biochemical alterations can be used as new endpoints. Comparable EC*x* values were achieved based on FTIR spectroscopy compared with traditional endpoints. The FTIR spectroscopy showed its ability to monitor effects in biochemical molecules such as proteins, lipids, DNA/RNA, and carbohydrates after exposure of duckweed to the chemicals at different levels.

Supplemental Data—The Supplemental Data are available on the Wiley Online Library at DOI: 10.1002/etc.3534.

Acknowledgment—The authors acknowledge financial support from the National Natural Science Foundation of China (grants U1133005 and U1401235) and the National Water Pollution Control Program of China (grant 2014ZX07206-005). Thanks also to J.Y. Li at Lancaster University for his assistance in biospectroscopy analysis. This is contribution number 2272 from GIG CAS.

Data Availability—Data, associated metadata, and calculation tools are available on request from the corresponding author (guang-guo.ying@gig.ac.cn; guangguo.ying@gmail.com).

REFERENCES

1. Blaauboer BJ, Boekelheide K, Clewell HJ, Daneshian M, Dingemans MM, Goldberg AM, Seibert H. 2012. The use of biomarkers of toxicity for integrating in vitro hazard estimates into risk assessment for humans. *Altex-Altern Anim Ex* 29:411–425.
2. Quinn B, Gagne F, Blaise C. 2008. An investigation into the acute and chronic toxicity of eleven pharmaceuticals (and their solvents) found in wastewater effluent on the cnidarian, *Hydra attenuata*. *Sci Total Environ* 389:306–314.
3. Yang LH, Ying GG, Su HC, Stauber JL, Adams MS, Binet MT. 2008. Growth-inhibiting effects of 12 antibacterial agents and their mixtures on the freshwater microalga *Pseudokirchneriella subcapitata*. *Environ Toxicol Chem* 27:1201–1208.
4. Adam O, Badot PM, Degiorgi F, Crini G. 2009. Mixture toxicity assessment of wood preservative pesticides in the freshwater amphipod *Gammarus pulex* (L.). *Ecotox Environ Safe* 72:441–449.
5. Bar-Ilan O, Albrecht RM, Fako VE, Furgeson DY. 2009. Toxicity assessments of multisized gold and silver nanoparticles in zebrafish embryos. *Small* 5:1897–1910.
6. Karami-Mohajeri S, Abdollahi M. 2011. Toxic influence of organophosphate, carbamate, and organochlorine pesticides on cellular metabolism of lipids, proteins, and carbohydrates: A systematic review. *Hum Exp Toxicol* 30:1119–1140.
7. Li J, Ying GG, Jones KC, Martin FL. 2015. Real-world carbon nanoparticle exposures induce brain and gonadal alterations in zebrafish (*Danio rerio*) as determined by biospectroscopy techniques. *Analyst* 140:2687–2695.
8. Wagner H, Liu Z, Langner U, Stehfest K, Wilhelm C. 2010. The use of FTIR spectroscopy to assess quantitative changes in the biochemical composition of microalgae. *J Biophotonics* 3:557–566.
9. Goormaghtigh E, Gasper R, Benard A, Goldsztein A, Raussens V. 2009. Protein secondary structure content in solution, films and tissues: Redundancy and complementarity of the information content in circular dichroism, transmission and ATR FTIR spectra. *BBA Proteins Proteom* 1794:1332–1343.
10. Vileno B, Jeney S, Sienkiewicz A, Marcoux PR, Miller LM, Forro L. 2010. Evidence of lipid peroxidation and protein phosphorylation in cells upon oxidative stress photo-generated by fullerols. *Biophys Chem* 152:164–169.
11. Baker MJ, Gazi E, Brown MD, Shanks JH, Gardner P, Clarke NW. 2008. FTIR-based spectroscopic analysis in the identification of clinically aggressive prostate cancer. *Brit J Cancer* 99:1859–1866.
12. Baker MJ, Gazi E, Brown MD, Shanks JH, Clarke NW, Gardner P. 2009. Investigating FTIR based histopathology for the diagnosis of prostate cancer. *J Biophotonics* 2:104–113.
13. Lewis PD, Lewis KE, Ghosal R, Bayliss S, Lloyd AJ, Wills J, Mur LA. 2010. Evaluation of FTIR spectroscopy as a diagnostic tool for lung cancer using sputum. *BMC Cancer* 10:1.
14. Ke Y, Li Y, Wang ZY. 2012. The changes of fourier transform infrared spectrum in rat brain. *J Forensic Sci* 57:794–798.
15. Llabjani V, Trevisan J, Jones KC, Shore RF, Martin FL. 2011. Derivation by infrared spectroscopy with multivariate analysis of bimodal contaminant-induced dose-response effects in MCF-7 cells. *Environ Sci Technol* 45:6129–6135.
16. Li J, Strong R, Trevisan J, Fogarty SW, Fullwood NJ, Jones KC, Martin FL. 2013. Dose-related alterations of carbon nanoparticles in mammalian cells detected using biospectroscopy: Potential for real-world effects. *Environ Sci Technol* 47:10005–10011.
17. Corte L, Tiecco M, Roscini L, Germani R, Cardinali G. 2014. FTIR analysis of the metabolomic stress response induced by N-alkyltropinium bromide surfactants in the yeasts *Saccharomyces cerevisiae* and *Candida albicans*. *Colloids Surf B* 116:761–771.
18. Corte L, Rellini P, Roscini L, Fatichenti F, Cardinali G. 2010. Development of a novel, FTIR (Fourier transform infrared spectroscopy) based, yeast bioassay for toxicity testing and stress response study. *Anal Chim Acta* 659:258–265.
19. Goormaghtigh E, Gasper R, Bénard A, Goldsztein A, Raussens V. 2009. Protein secondary structure content in solution, films and tissues: Redundancy and complementarity of the information content in circular dichroism, transmission and ATR FTIR spectra. *BBA Proteins Proteom* 1794:1332–1343.
20. Miller LM, Dumas P. 2010. From structure to cellular mechanism with infrared microspectroscopy. *Curr Opin Struct Biol* 20:649–656.
21. Martin FL, Kelly JG, Llabjani V, Martin-Hirsch PL, Patel, II, Trevisan J, Fullwood NJ, Walsh MJ. 2010. Distinguishing cell types or populations based on the computational analysis of their infrared spectra. *Nat Protoc* 5:1748–1760.
22. Baker MJ, Trevisan J, Bassan P, Bhargava R, Butler HJ, Dorling KM, Fielden PR, Fogarty SW, Fullwood NJ, Heys KA, Hughes C, Lasch P, Martin-Hirsch PL, Obinaju B, Sockalingum GD, Sule-Suso J, Strong RJ, Walsh MJ, Wood BR, Gardner P, Martin FL. 2014. Using Fourier transform IR spectroscopy to analyze biological materials. *Nat Protoc* 9:1771–1791.
23. Liland KH. 2011. Multivariate methods in metabolomics—From preprocessing to dimension reduction and statistical analysis. *Trac-Trend Anal Chem* 30:827–841.
24. Harvey TJ, Gazi E, Henderson A, Snook RD, Clarke NW, Brown M, Gardner P. 2009. Factors influencing the discrimination and classification of prostate cancer cell lines by FTIR microspectroscopy. *Analyst* 134:1083–1091.
25. Van Dam RA, Camilleri C, Turley C, Binet MT, Stauber JL. 2004. Chronic toxicity of the herbicide tebuthiuron to the tropical green alga *Chlorella* sp. and the duckweed *Lemna aequinoctialis*. *Australas J Ecotoxicol* 10:97–104.
26. Kolthoff IM, Chantooni MK Jr. 1972. A critical study involving water, methanol, acetonitrile, N, N-dimethylformamide, and dimethyl sulfoxide of medium ion activity coefficients, γ, on the basis of the γ AsPh4+=γ BPh4- Assumption. *J Phys Chem* 76:2024–2034.
27. Lichtenthaler HK, Buschmann C. 2001. Chlorophylls and carotenoids: Measurement and characterization by UV-VIS spectroscopy. *Curr Protoc Food Anal Chem* F4.3.1–F4.3.8.
28. Trevisan J, Angelov PP, Scott AD, Carmichael PL, Martin FL. 2013. IRootLab: A free and open-source MATLAB toolbox for vibrational biospectroscopy data analysis. *Bioinformatics* 29:1095–1097.
29. Villalba SD, Cunningham P. 2008. An evaluation of dimension reduction techniques for one-class classification. *Artif Intell Rev* 27:273–294.
30. Trevisan J, Angelov PP, Patel, II, Najand GM, Cheung KT, Llabjani V, Pollock HM, Bruce SW, Pant K, Carmichael PL, Scott AD, Martin FL. 2010. Syrian hamster embryo (SHE) assay (pH 6.7) coupled with infrared spectroscopy and chemometrics towards toxicological assessment. *Analyst* 135:3266–3272.
31. Douglas MP, Rogers SO. 1998. DNA damage caused by common cytological fixatives. *Mutat Res* 401:77–88.
32. Dwyer DS, Bradley RJ. 2000. Chemical properties of alcohols and their protein binding sites. *Cell Mol Life Sci* 57:265–275.
33. Ali Jamal A, Abd El-Aziz GS, Hamdy RM, Al-Hayani A, Al-Maghrabi J. 2014. The innovative safe fixative for histology, histopathology, and immunohistochemistry techniques: Pilot study using shellac alcoholic solution fixative. *Microsc Res Tech* 77:385–393.
34. Young G, Nippgen F, Titterbrandt S, Cooney MJ. 2010. Lipid extraction from biomass using co-solvent mixtures of ionic liquids and polar covalent molecules. *Sep Purif Technol* 72:118–121.

35. Kiernan JA. 2000. Formaldehyde. Formalin, paraformaldehyde and glutaraldehyde: What they are and what they do. *Microsc Today* 8:8–12.
36. Häensch R, Mendel RR. 2009. Physiological functions of mineral micronutrients (Cu, Zn, Mn, Fe, Ni, Mo, B, Cl). *Curr Opin Plant Biol* 12: 259–266.
37. Bremner I. 1998. Manifestations of copper excess. *Am J Clin Nutr* 67:1069S–1073S.
38. Gaetke LM, Chow CK. 2003. Copper toxicity, oxidative stress, and antioxidant nutrients. *Toxicology* 189:147–163.
39. Schützendübel A, Polle A. 2002. Plant responses to abiotic stresses: Heavy metal-induced oxidative stress and protection by mycorrhization. *J Exp Bot* 53:1351–1365.
40. Ouzounidou G. 1994. Copper-induced changes on growth, metal content and photosynthetic function of *Alyssum montanum L.* plants. *Environ Exp Bot* 34:165–172.
41. Shah K, Kumar RG, Verma S, Dubey RS. 2001. Effect of cadmium on lipid peroxidation, superoxide anion generation and activities of antioxidant enzymes in growing rice seedlings. *Plant Sci* 161:1135–1144.
42. Chaoui A, Mazhoudi S, Ghorbal MH, Ferjani EE. 1997. Cadmium and zinc induction of lipid peroxidation and effects on antioxidant enzyme activities in bean (*Phaseolus vulgaris L.*). *Plant Sci* 127: 139–147.
43. Schutzendubel A, Schwanz P, Teichmann T, Gross K, Langenfeld-Heyser R, Godbold DL, Polle A. 2001. Cadmium-induced changes in antioxidative systems, hydrogen peroxide content, and differentiation in scots pine roots. *Plant Physiol* 127:887–898.
44. Romero-Puertas MC, Palma JM, Gómez M, Del Rio LA, Sandalio LM. 2001. Cadmium causes the oxidative modification of proteins in pea plants. *Plant Cell Environ* 2002:5.
45. Fang XQ, Deng ZP, Huo LH, Wan W, Zhu ZB, Zhao H, Gao S. 2011. New family of silver(I) complexes based on hydroxyl and carboxyl groups decorated arenesulfonic acid: Syntheses, structures, and luminescent properties. *Inorg Chem* 50:12562–12574.
46. Nwani CD, Lakra WS, Nagpure NS, Kumar R, Kushwaha B, Srivastava SK. 2010. Toxicity of the herbicide atrazine: Effects on lipid peroxidation and activities of antioxidant enzymes in the freshwater fish *Channa punctatus* (Bloch). *Int J Environ Res Public Health* 7:3298–3312.
47. Tan W, Li Q, Zhai H. 2012. Photosynthesis and growth responses of grapevine to acetochlor and fluoroglycofen. *Pestic Biochem Phys* 103:210–218.